Direct Numerical Solution Of The Boltzmann Equation

Felix Tcheremissine

Dorodnicyn Computing Center of RAS, 119991, GSP-1, 40 Vavilov str., Moscow, Russia

Abstract. Progress in computer hardware and improvement of numerical methods made solution of the Boltzmann equation for rather complex gas dynamic problems real. The method developed by the author is based on a projection technique for evaluation of the collision operator. The computed collision integral is conservative by density, impulse, and energy, and became equal to zero when the solution has a form of the Maxwellian distribution. The later feature sharply increases its efficiency, especially for the near equilibrium flows. The method is extended on a mixture of gases and the gases with internal degrees of freedom, where it can incorporate real physical parameters of molecular potential and of internal energy spectrum. Examples of computations for a range of Mach and Knudsen numbers are presented.

INTRODUCTION

Solution of the Boltzmann equation was initiated by Nordsieck's group in Illinois, USA nearly 40 years ago when first big computers have appeared [1]. In this method velocity space was divided by equal cells, and collision integrals were evaluated by simulating of molecular collisions with randomly chosen velocity vectors. Then computed mean values per a cell were attributed to the middle points of the cells, and the obtained system of equations was solved by an iterative method. A few years later another method in which the collision integrals were evaluated directly at the nodes of the grid in the velocity space by Monte Carlo technique was developed by the author of this paper [2]. Very soon the main deficiency of both approaches – non-fulfillment of conservation laws in the computed integrals - became evident. In [3], a splitting finite-difference scheme for the kinetic equation has been proposed, and then a special correction was developed to satisfy the conservation laws at the relaxation stage [4]. The new method showed itself much more efficient then that of [2], but the correction introduced some additional numerical viscosity, and required artificial assumptions in the case of gas mixtures [5, 6]. The next step in the development of conservative methods has been made after construction of a Discrete Velocity Model [7]. In this model molecular velocities are given at a uniform Cartesian lattice and impact parameters of a molecular collision are such that post collision velocities belong to the same grid. Therefore, it imposes a restriction on impact parameters, which are independent in the true Boltzmann equation. Based on a similar idea, conservative methods for the Boltzmann collision integrals have been proposed [8, 9].

The conservative method without any selection of impact parameters has been developed by the author [10, 11]. It was then improved and adopted for computing near equilibrium flows [12, 13], extended to gas mixtures [14], and gases with internal degrees of freedom [15]. The main features of the method are described bellow.

NUMERICAL METHOD

Consider the Boltzmann equation

$$\partial f / \partial t + \xi \cdot \partial f / \partial x = I$$

It is solved at a grid of N_0 equidistant nodes ξ_γ with a step $\boldsymbol{h}$ confined in a domain Ω of a volume V. On the basis of Dirac's δ–functions, the distribution function and the collision integral can be presented in a form

$$f(\xi,x,t)=\sum_{\gamma=1}^{N_0} f_\gamma(x,t)\delta(\xi-\xi_\gamma),\ I(\xi,x,t)=\sum_{\gamma=1}^{N_0} I_\gamma(x,t)\delta(\xi-\xi_\gamma) \qquad (1)$$

CP762, *Rarefied Gas Dynamics: 24th International Symposium,* edited by M. Capitelli

Report Documentation Page

Form Approved
OMB No. 0704-0188

1. REPORT DATE	2. REPORT TYPE	3. DATES COVERED
13 JUL 2005	**N/A**	**-**

4. TITLE AND SUBTITLE	5a. CONTRACT NUMBER
Direct Numerical Solution Of The Boltzmann Equation	5b. GRANT NUMBER
	5c. PROGRAM ELEMENT NUMBER
6. AUTHOR(S)	5d. PROJECT NUMBER
	5e. TASK NUMBER
	5f. WORK UNIT NUMBER
7. PERFORMING ORGANIZATION NAME(S) AND ADDRESS(ES) **Dorodnicyn Computing Center of RAS, 119991, GSP-1, 40 Vavilov str., Moscow, Russia**	8. PERFORMING ORGANIZATION REPORT NUMBER
9. SPONSORING/MONITORING AGENCY NAME(S) AND ADDRESS(ES)	10. SPONSOR/MONITOR'S ACRONYM(S)
	11. SPONSOR/MONITOR'S REPORT NUMBER(S)

12. DISTRIBUTION/AVAILABILITY STATEMENT
Approved for public release, distribution unlimited

13. SUPPLEMENTARY NOTES
See also ADM001792, International Symposium on Rarefied Gas Dynamics (24th) Held in Monopoli (Bari), Italy on 10-16 July 2004.

14. ABSTRACT

15. SUBJECT TERMS

16. SECURITY CLASSIFICATION OF:			17. LIMITATION OF ABSTRACT	18. NUMBER OF PAGES	19a. NAME OF RESPONSIBLE PERSON
a. REPORT **unclassified**	b. ABSTRACT **unclassified**	c. THIS PAGE **unclassified**	**UU**	**9**	

In configuration space, an arbitrary discrete grid x_i can be applied. When the coefficients of expansions (1) are determined, the problem reduces to the solution by a finite-difference method of a set of equations

$$\partial f_\gamma / \partial t + \xi_\gamma \cdot \partial f_\gamma / \partial x = I_\gamma \tag{2}$$

Evaluation Of The Collision Integral

Let us write the Boltzmann collision integral for a mono atomic gas, omitting the variables x and t, in a form

$$I(\xi) \equiv I[f(\xi)] = \int_{-\infty}^{\infty} \int_0^{2\pi} \int_0^{b_m} (f' f_*' - f f_*) g b db d\varphi d\xi_*$$

where velocities after collision ξ', ξ_*' are related to those before the collision by the formulae

$$\xi' = \xi + k(k \cdot g),\ \xi_*' = \xi_* - k(k \cdot g),\quad g = \xi_* - \xi \tag{3}$$

The integral possesses the following properties that should be taken into account

$$\int_{-\infty}^{\infty} I(\xi)\psi(\xi) d\xi = 0, \quad \psi(\xi) = \{1, \xi, \xi^2\} \tag{4}$$

$$I[f_M] = 0\ , \qquad f_M = n\left(\frac{m}{2\pi kT}\right)^{\frac{3}{2}} \exp\left(-\frac{m(\xi - \xi_0)^2}{2kT}\right) \tag{5}$$

The condition (4) leads to correct hydrodynamic equations, and the fulfillment of (5) by a numerical method increases the accuracy of the method in near equilibrium regimes where the solution is close to a Maxwellian.

The collision integral at a point ξ^* can be presented in a form

$$I(\xi^*) = \int_{-\infty}^{\infty} \int_{-\infty}^{\infty} \int_0^{2\pi} \int_0^{b_m} \delta(\xi - \xi^*)(f' f_*' - f f_*) g b db d\varphi d\xi_* d\xi$$

Let us take $\xi^* = \xi_\gamma$, denote $\phi(\xi_\gamma) = \delta(\xi - \xi_\gamma) + \delta(\xi_* - \xi_\gamma) - \delta(\xi' - \xi_\gamma) - \delta(\xi'_* - \xi_\gamma)$ and write the integral in a symmetric form

$$I_\gamma = \frac{1}{4} \int_{-\infty}^{\infty} \int_{-\infty}^{\infty} \int_0^{2\pi} \int_0^{b_m} \phi(\xi_\gamma)(f' f_*' - f f_*) g b db d\varphi d\xi_* d\xi \tag{6}$$

For evaluation of the integral (6) consider a domain $\Omega \times \Omega \times 2\pi \times b_m$ in which we introduce a uniform integration grid $\xi_{\alpha_\nu}, \xi_{\beta_\nu}, b_\nu, \varphi_\nu$ with N_ν nodes, such that ξ_{α_ν} and ξ_{β_ν} coincide with the velocity grid, and exclude all values of variables b_ν, φ_ν for which post collision velocities $\xi'_{\alpha_\nu}, \xi'_{\beta_\nu}$ fall outside of Ω. Because the points $\xi'_{\alpha_\nu}, \xi'_{\beta_\nu}$, in general case don't coincide with the velocity grid nodes, a regularization of (6) is needed.

Let ξ_{λ_ν} and ξ_{μ_ν} denote the nearest vertices of cells inside which ξ'_{α_ν} and ξ'_{β_ν} lie, and $\xi_{\lambda_\nu + s}$ and $\xi_{\mu_\nu - s}$ denote a pair of other vertices that are located symmetrically at the opposite side of a collision sphere presented in **Figure 1**.

Two ways of the regularization define two versions of the method of evaluation of the collision integral.

First Version: Conservative Method With Exact Asymptotic

Let us replace the two last δ –functions in $\phi(\xi_\gamma)$ by the expressions

$$\delta(\xi'_{\alpha_\nu} - \xi_\gamma) = (1 - r_\nu)\delta(\xi_{\lambda_\nu} - \xi_\gamma) + r_\nu \delta(\xi_{\lambda_\nu + s} - \xi_\gamma),\ \delta(\xi'_{\beta_\nu} - \xi_\gamma) = (1 - r_\nu)\delta(\xi_{\mu_\nu} - \xi_\gamma) + r_\nu \delta(\xi_{\mu_\nu - s} - \xi_\gamma)$$

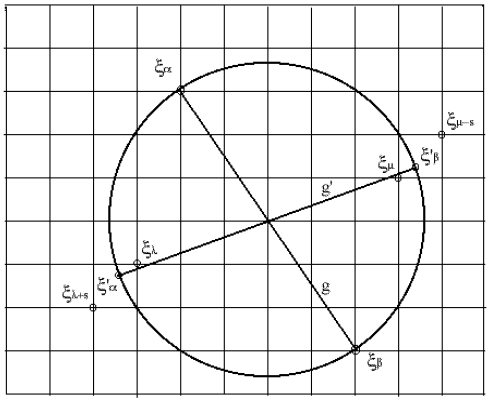

FIGURE 1. Scheme of an Elastic Collision

This means that contributions to the points $\xi'_{\alpha_\nu}, \xi_{\beta_\nu}'$ are distributed between the neighboring nodes. Denote $E_0 = (\xi'_{\alpha_\nu})^2 + (\xi'_{\beta_\nu})^2$, $E_1 = (\xi_{\lambda_\nu})^2 + (\xi_{\mu_\nu})^2, E_2 = (\xi_{\lambda_\nu+s})^2 + (\xi_{\mu_\nu-s})^2$. One of conditions $E_1 \le E_0 < E_2$, or $E_2 < E_0 \le E_1$ is true. The coefficient r_ν is defined by the energy conservation law $E_0 = (1-r_\nu)E_1 + r_\nu E_2$, from which it follows that $0 \le r_\nu < 1$. The value of $f'_{\alpha_\nu} f'_{\beta_\nu}$ can be defined by interpolation. It follows from the definition of the coefficient r_ν that the following formula is exact, when $f_\beta = f_M(\xi_\beta)$ at all the grid nodes

$$f'_{\alpha_\nu} f'_{\beta_\nu} = (f_{\lambda_\nu} f_{\mu_\nu})^{1-r_\nu} \cdot (f_{\lambda_\nu+s} f_{\mu_\nu-s})^{r_\nu} \tag{7}$$

The integral (6) is evaluated as a sum simultaneously in all the nodes ξ_γ of the velocity grid. With $B = V\pi b_m^2/(4N_c), N_c = N_\nu / N_0$, $\Delta_\nu = (f_{\alpha_\nu} f_{\beta_\nu} - f'_{\alpha_\nu} f'_{\beta_\nu}) g_\nu b_\nu$, and Kronnecker's symbol $\delta_{\gamma,\beta}$, one obtains

$$I_\gamma = B\sum_{\nu=1}^{N_\nu} [-(\delta_{\gamma,\alpha_\nu} + \delta_{\gamma,\beta_\nu}) + (1-r_\nu)(\delta_{\gamma,\lambda_\nu} + \delta_{\gamma,\mu_\nu}) + r_\nu(\delta_{\gamma,\lambda_\nu+s} + \delta_{\gamma,\mu_\nu-s})]\Delta_\nu, \tag{8}$$

In this method the conditions (4) and (5) are fulfilled exactly for each contribution in the sum.

Second Version: Conservative Method Without Interpolation

Divide the integral (6) into two parts: the one containing ff_*, which gives the contribution of "direct" collisions, and that with $f'f'_*$, which describes "inverse" collisions. In the first part, we apply the same projection function $\phi(\xi_\gamma)$. In the second part, we replace the kernel by

$$\{[\delta(\xi_{\alpha_\nu} - \xi_\gamma) + (\xi_{\beta_\nu} - \xi_\gamma)][(1-r_\nu^*) f_{\lambda_\nu} f_{\mu_\nu} + r_\nu^* f_{\lambda_\nu+s} f_{\mu_\nu-s}] +$$
$$[\delta(\xi_{\lambda_\nu} - \xi_\gamma) + (\xi_{\mu_\nu} - \xi_\gamma)](1-r_\nu^*) f_{\lambda_\nu} f_{\mu_\nu} + [\delta(\xi_{\lambda_\nu+s} - \xi_\gamma) + \delta(\xi_{\mu_\nu-s} - \xi_\gamma)] r_\nu^* f_{\lambda_\nu+s} f_{\mu_\nu-s}\} g_\nu b_\nu .$$

The coefficient r_ν^* is found from the energy conservation law that gives $r_\nu^* = r_\nu \Delta_\nu^{(1)} / [r_\nu \Delta_\nu^{(1)} + (1-r_\nu)\Delta_\nu^{(2)}]$, where $\Delta_\nu^{(1)} = f_{\lambda_\nu} f_{\mu_\nu}$, and $\Delta_\nu^{(2)} = f_{\lambda_\nu+s} f_{\mu_\nu-s}$. Denote $\Delta_\nu^{(0)} = f_{\alpha_\nu} f_{\beta_\nu}$. The collision integral has the form

$$I_\gamma = B\sum_{\nu=1}^{N_\nu} \{(\delta_{\alpha_\nu,\gamma} + \delta_{\beta_\nu,\gamma})[(1-r_\nu^*)\Delta_\nu^{(1)} + r_\nu^*\Delta_\nu^{(2)} - \Delta_\nu^{(0)}] + (\delta_{\lambda_\nu,\gamma} + \delta_{\mu_\nu,\gamma})[(1-r_\nu)\Delta_\nu^{(0)} - (1-r_\nu^*)\Delta_\nu^{(1)}]$$
$$+ (\delta_{\lambda_\nu+s,\gamma} + \delta_{\mu_\nu-s,\gamma})[r_\nu\Delta_\nu^{(0)} - r_\nu^*\Delta_\nu^{(2)}]\} b_\nu g_\nu \tag{9}$$

In this version, the condition (5) is fulfilled with the accuracy of the order of $O(h)$ for each contribution to the integral (9). The accuracy for the whole integral tends to $O(h^2)$ when $N_\nu \to \infty$. Compared with the first version, the integral doesn't contain numerical diffusion induced by the interpolation. Numerical experiments have shown

that for most cases, except of the near equilibrium flows, the last method is more efficient. In particular, it permits calculations with a coarse mesh in velocity space. The switching between the two versions, if needed, is very easy.

Both methods are very economic in terms of arithmetic operations, because calculation of r_ν, g_ν, b_ν and of numbers of the functions $f_{\alpha_\nu}, f_{\beta_\nu}, f_{\lambda_\nu}, f_{\mu_\nu}, f_{\lambda_\nu+s}, f_{\mu_\nu-s}$ in the array of the distribution function can be made in advance and then used for all nodes by physical space. Classical molecular potentials can be applied without substantial slowing down of the computation, and there is no need for artificial molecular models. The 8-dimensional integration grid is build by the method [16] with an error estimate about $O(N_\nu^{-1})$ versus $O(N_\nu^{-0.5})$ for a Monte Carlo grid.

Remark There is another way to satisfy the conditions (4) and (5): select ξ_{λ_ν} and ξ_{μ_ν} as the pair of the nearest nodes on the sphere. However, the approximation of real collisions in this case is quite suspicious.

Extension For Gas Mixtures And Inelastic Collisions

A transformation of the collision integral in impulse space $(\xi, \xi_*) \to (p, p_*)$ is sufficient for extension of the method for a mixture of gases [10, 11]. Although the scheme of **Figure 1** is no more valid, the post collision impulses $p'_{\alpha_\nu}, p'_{\beta_\nu}$ lie symmetrically against corresponding nearest grid nodes $p_{\lambda_\nu}, p_{\mu_\nu}$, and $p_{\lambda_\nu+s}, p_{\mu_\nu-s}$, because the increment of the impulse can be presented as $\delta p_{\alpha\beta} = (k + \delta')h$, with an integer vector k and $|\delta'| < 1$.

The formulae for the collision integral (8) and (9), as well as the expressions of the splitting coefficients r and r^* through the energies remain the same. The realization of the method for a binary gas mixture has been done in [14]. The case of inelastic collisions in a gas with internal degrees of freedom was considered in [15] in the framework of Wang Chang – Uhlenbeck kinetic equation [17]

$$\partial f_i / \partial t + \xi_i \partial f / \partial x = \sum_{j,k,l} \int_{-\infty}^{\infty} \int_0^{2\pi} \int_0^{b_m} (f_k f_l - f_i f_j) P_{ij}^{kl} g_{ij} b db d\varphi d\xi_j \qquad (10)$$

Here P_{ij}^{kl} is a probability of transition from the energy levels (***i, j***) to (***k, l***), and f_i is the velocity distribution function for the level ***i***. In impulse space, kinetic equations for binary reacting mixtures have the same form.

Finite-Difference Scheme

The set of N_0 equations (2) is solved by the splitting method with a time step $\tau = t^{j+1} - t^j$

$$\partial f_\gamma^* / \partial t + \xi_\gamma \partial f_\gamma^* / \partial x = 0, \quad f_\gamma^{*,j} = f_\gamma^j \qquad (11)$$

$$\partial f_\gamma / \partial t = I_\gamma, \quad f_\gamma^j = f_\gamma^{*,j+1} \qquad (12)$$

The equation (11) is approximated by a second order explicit flux conservative scheme. To make the splitting scheme symmetric, the solution of (11) is repeated twice at a half-interval of τ that improves the accuracy and permits to attenuate the Courant condition. For the equation (12), different methods, including second order predictor-corrector scheme, and solution of an integral equation were tested. The last scheme is written in the form

$$f_\gamma^{j+1} = f_\gamma^j + \int_{t^j}^{t^{j+1}} I(t) dt$$

By introducing the variable $t_\nu = \tau\nu / N_\nu$ and an intermediate solution $f_\gamma^{j+\nu/N_\nu}$, one obtains the scheme

$$f_\gamma^{j+\nu/N_\nu} = f_\gamma^{j+(\nu-1)/N_\nu} + \tau \cdot \Delta_{\gamma,\nu}^{j+(\nu-1)/N_\nu},$$

where $\Delta_{\gamma,\nu}^{j+(\nu-1)/N_\nu}$ is the ν-th term of the sums (8) or (9). The calculation of the collision integral is replaced by continuous updating of the distribution function at the relaxation stage that is convenient in realization.

To resolve fast kinetic processes, the condition $\tau < \tau_0$, where τ_0 is the time between collisions, should be satisfied. The size of the mesh in configuration space can vary and exceed the local mean free path (m.f.p.).

EXAMPLES OF COMPUTATIONS

Selected examples bellow illustrate the performance of the approach for different ranges of physical parameters, rather than study in details particular gas flows. To avoid unnecessary complications, simple geometries of the flow are considered. In all cases, boundary conditions at the surface are formulated as perfect accommodation with reflected Maxwellian function. The computations are made on a 2.6 Ghz Pentium-4 PC.

Near Equilibrium and Low Speed Flows

This case is the mast favorable for application of the developed method by two reasons. First, the solution in this case is close to a Maxwellian function, and therefore its principal part is evaluated exactly in the collision integral. Second, the needed area of the velocity space is relatively small that permits using a small number of velocity grid nodes N_0.

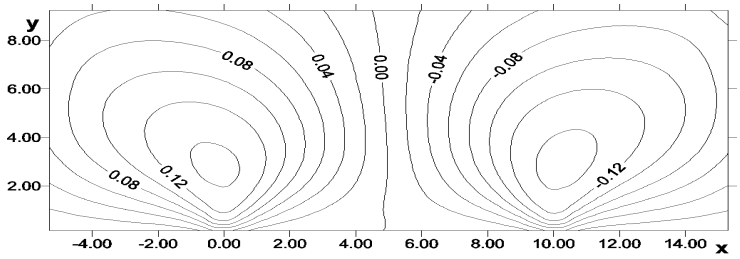

FIGURE 2. Low Speed Flow Along a Plate

In **Figure 2,** the transversal velocity in units of $10^3 v$ is shown for a hard-sphere gas flow along a cold plate with incoming Mach number **M=0.001** and Knudsen number **Kn=0.1**. The plate is located between $x = 0$ and $x = 10$, in dimensionless units expressed in terms of the m.f.p. The velocity is in units of $(kT_0 / m)^{1/2}$. The velocities as low as 10^{-5} are captured without problems. The computation until $t = 100\tau_0$ took about **15 min** of CPU time and use**13 MB** of computer memory. For this case, the first method of calculation of the collision integral had advantage over the second one, but for **M>0.02** both versions became equally efficient.

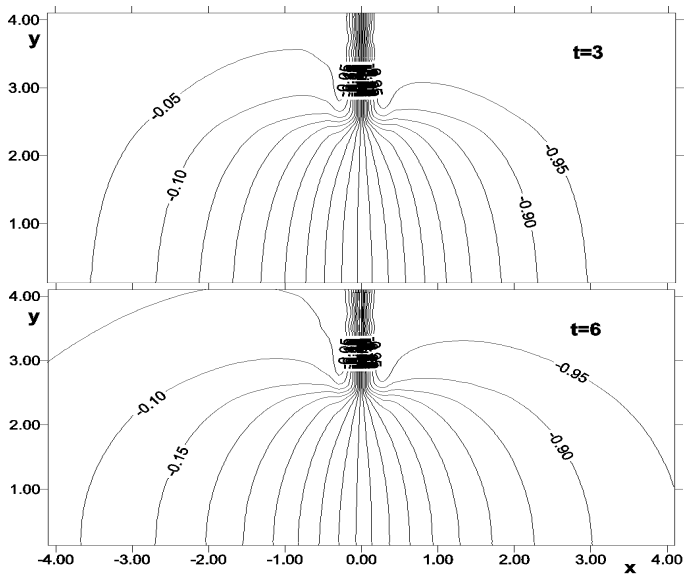

FIGURE 3. Unsteady Flow through a Quadratic Orifice

Figure 3 presents a 3D simulation of unsteady flow through a quadratic orifice for a density ratio $n_0 / n_1 = 0.995$, where n_1 is the density in the left vessel, and n_0 is that at the right side of the wall. The gas temperatures are equal at both sides. The Knudsen number defined by the orifice side length is **Kn=0.2**. Deviations of density multiplied by **200** in the longitudinal plane $z = 0$ are shown at two moments of time measured in units of τ_0. The orifice is located at $x = 0$. The problem is solved for a gas with a **-12** exponential potential. The number of nodes in configuration space is **12000**, the number of velocity nodes is **4224**, computer memory usage is **200 MB,** and the CPU time per τ_0 is **8 min**.

Hypersonic Flows

Consider now the opposite case of big gradients and high deviations from the thermodynamic equilibrium state. In **Figure 4, the** density and temperature fields for a 2D flow of a hard-sphere gas are presented along a cold plane plate for **M=10** and **Kn=0.01**. The plate is located along the ***x*** axis with the leading edge at ***x*=0**. All distances are measured in the units of the m.f.p. of the incoming flow, and flow parameters are related to their unperturbed values.

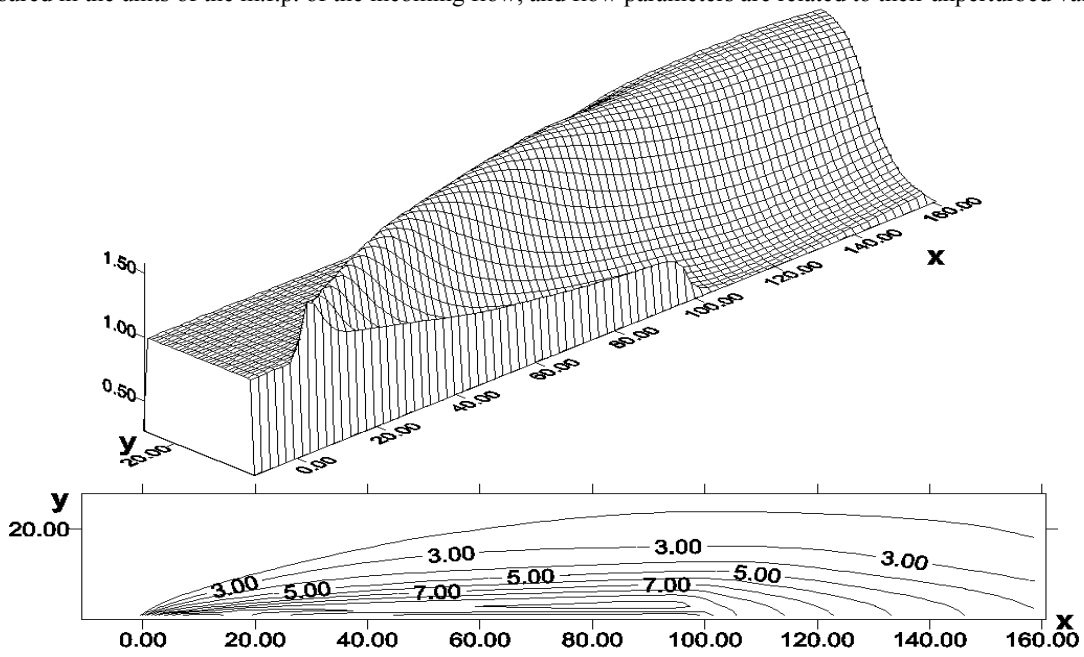

FIGURE 4. Hypersonic Flow along a Plate. The Density Field (Top) and the Temperature Field (Bottom)

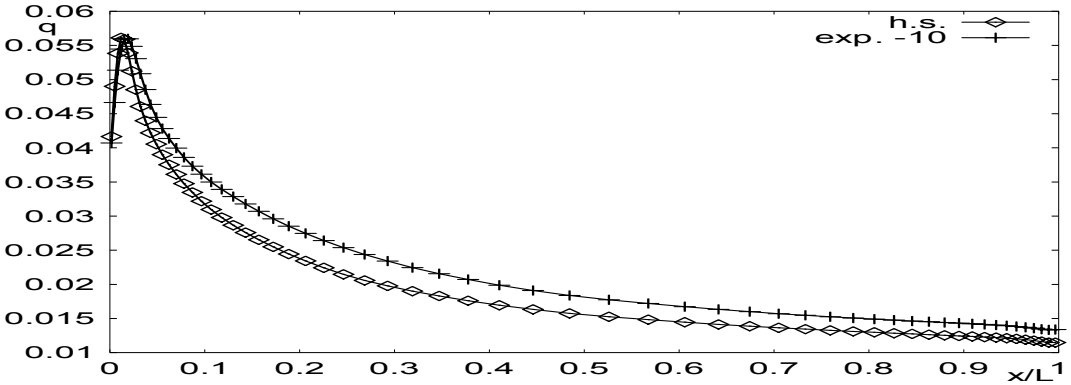

FIGURE 5. Hypersonic Flow along a Plate. Local Energy Flux for Two Molecular Models

The computation is made with **5400** nodes in configuration space, **2808** nodes in velocity space, with total memory usage of about **120 MB**, and CPU time about **3h**. The test computation with **5768** velocity nodes gave practically the same result with maximal deviations of local heat and drag at the plate of **6%**. In **Figure 5, the** normalized by $u_0^3/2$ energy flux to the plate is presented for two molecular models. For correct computation of aerodynamic reactions, variable mesh in ***x*** and ***y*** directions were used. The mesh size along the ***y*** axis near the plate and along the ***x*** axis near the edges of the plate were equal to about **0.2** of the m.f.p.

In **Figure 6,** the density along the symmetry line is shown for a 2D planar flow around an orthogonal thin plate with the frontal side temperature $T_f = 2$ and the rear side temperature $T_r = 1$ for **M=8** and **Kn=0.05**. The flow is characterized by the formation of a sharp Knudsen layer in front of the plate and considerable rarefaction behind the plate and require the application of variable mesh condensed near the plate. The mesh size along the ***x*** axis near the plate was equal to **0.05** of the m.f.p. The stabilization of the solution behind the plate required quite a long time of calculation.

This example demonstrates the ability of the method for computing flows with strong spatial variations of hydrodynamic parameters.

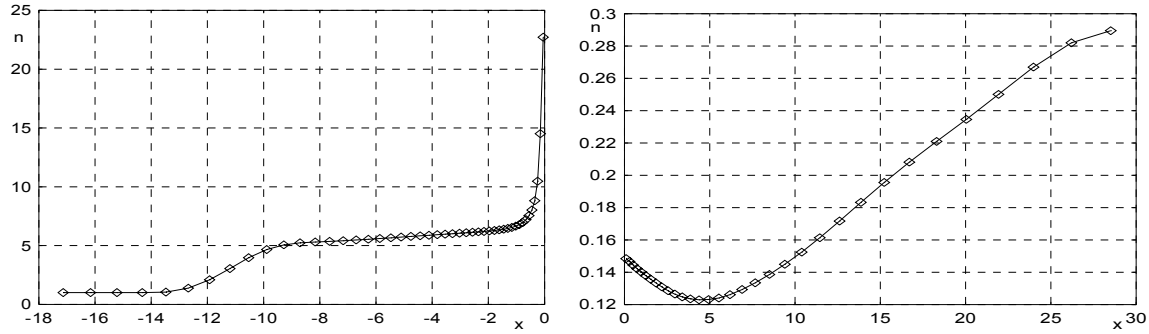

FIGURE 6. Hypersonic Flow around an Orthogonal Plate. Density at Both Sides of the Plate at ***x*=0**

Gas Flows With Internal Degrees of Freedom

As an example of gas flows with internal degrees of freedom consider a shock wave structure in Nitrogen at room temperature for **M=2**, for which it exists experimental data [18]. The data of rotational spectrum and the Lennard-Jones potential for Nitrogen were taken from [19, 20], and the R-T cross sections are from [21, 22]. In **Figure 7,** the normalized translational, rotational, and longitudinal temperatures are shown. In **Figure 8,** the degenerated rotational spectrum (populations of the levels) at 5 positions is reported, including equilibrium spectrum before the shock wave at ***x*=-12**, and behind the wave at ***x*=12**. **Figure 9** presents the comparison of computed and experimental densities.

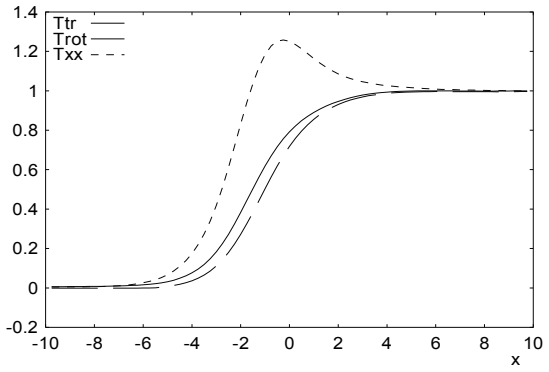

FIGURE 7. Temperatures

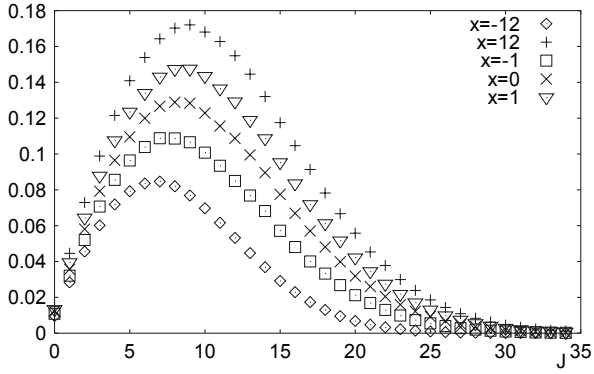

FIGURE 8. Rotational Spectrum

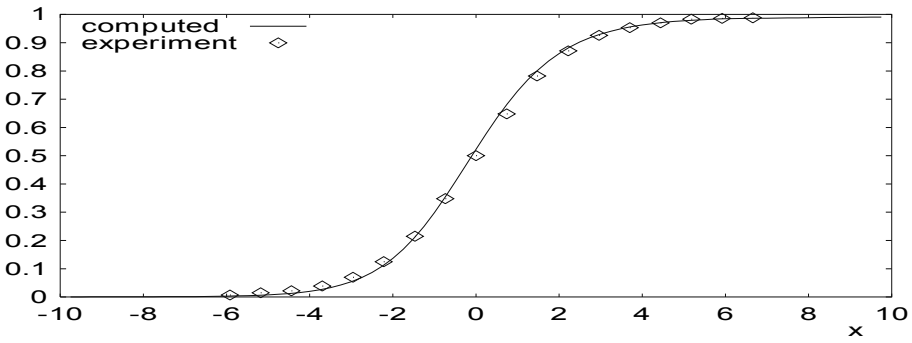

FIGURE 9. Comparison of Computed and Measured Densities

The computations were made for **35** degenerated energy levels and require about **32 MB** of memory.

ACKNOWLEDGMENTS

The support of the grant N 04-01-00347 of Russian Federation for Basic Research is acknowledged.

REFERENCES

1. Nordsieck, A., and Hicks, B.L., "Monte Carlo evaluation of the Boltzmann collision integral", in Rarefied Gas Dynamics, Proc. 5-th Intern. Symposium on RGD, edited by C.L.Brundin, Plenum Press, N.Y-L., 1967, pp. 695-710.
2. Cheremisin, F.G., USSR Comput. Maths. Math. Phys., 10 (3), pp. 654-665, (1970)
3. Aristov, V.V., and Cheremisin, F.G., Doklady Acad. of Sc. of USSR, 231 (1), pp. 49-52, (1976).
4. Aristov, V.V., and Tcheremissine F.G., USSR Comput. Maths. Math. Phys., 20 (1), pp.191-207, (1980)
5. Mausbach, P., and Beylich, A.E., " Numerical solution of the Boltzmann equation for one-dimensional problems in binary mixtures", in Proc. 13-th Intern. Symp. on RGD, edited by Belotzerkovskii O.M. et all, Plenum Press, N.Y-L., 1985, pp. 285-293.
6. Raines, A.A., " Numerical solution of the Boltzmann equation for one dimensional problem in a binary gas mixture", in Proc. 17-th Intern Symp. on RGD, edited by A.E.Beylich, Weinheim,N.-Y.,1991, pp.328-331.
7. Inamuro, T., and Sturtevant, B., Phys. Fluids, A 2, pp. 2196-2203, (1990)
8. Rogier, F., and Schneider, J.A., Transport Theory Stat. Phys., 23 (1-3), pp.313-338, (1994)
9. Buet, C., "A discrete velocity scheme for the Boltzmann operator of rarefied gas dynamics", Rarefied Gas Dynamics 19, edited by J. Harvey and G. Lord, Oxford Science Publications, 1995, 2. pp. 878-884.
10. Tcheremissine, F.G., "Conservative discrete ordinates method for solving Boltzmann kinetic equation", Communications on Applied Mathematics, Computing Center of the Russian Academy of Sciences, Moscow, 1996, P.50.
11. Tcheremissine, F.G., "Conservative Discrete Ordinates Method for Solving of Boltzmann Kinetic Equation", in Rarefied Gas Dynamics 20, edited by Ching Shen, Peking University Press, Beyjing, China, 1997, pp. 297-302.
12. Cheremisin, F.G., Doklady Physics, 45 (8), pp. 401-404, (2000)
13. Tcheremissine, F.G., "Solution of the Boltzmann Equation in Stiff Regime", in Intern. Series of Numerical Mathematics, Birkhauser Verlag, Basel, Switzerland, 2001, 141, pp. 884-890.
14. Raines, A., Eur. J. Mech. B Fluids 21, pp. 599-610, (2002)
15. Cheremisin, F.G., Doklady Physics, 47 (12), pp. 872-875, (2002)
16. Korobov, N. N., Trigonometric Suns and Their Applications, Mir, Moscow, 1989
17. Ferziger, J.H, and Kaper, H.J., Mathematical Theory of Transport Processes in Gases, North-Holland. Publ. Company, Amsterdam, 1972; Mir, Moscow, 1976.
18. Alsmeyer, H., J.Fluid Mech., 74, pp. 497-513, (1976)
19. Hirschfelder, J.O., Curtiss, C.F., and Bird, R.B., Molecular Theory of Gases and Liquids, Wiley, N.-Y., 1954.
20. Landau, L.D., and Lifshitz, E.M., Course of Theoretical Physics, Vol.5: Statistical Physics. Pergamon Press, Oxford, 1977; Nauka, Moscow, 1995.
21. Beylich, A.E., An Interlaced System for Nitrogen Gas, Technische Hochschule Aachen, 2000, P.14.
22. Bartels, C., and Beylich, A.E., "Rotational Energy Transfer and Dimerisation in Nitrogen", in Rarefied Gas Dynamics 20, edited by Ching Shen, Peking University Press, Beyjing, China, 1997, pp. 749-754.

Appendix: Output Of The Distribution Function

As a supplement for the analysis that was made at the level of hydrodynamic parameters, we present the distribution function for the considered hypersonic flow about the orthogonal plate (contours at the top, and the surface at the bottom). Note the part of the distribution that presents molecules going to the plate (at the left), and a spread of the function in ξ_y direction.

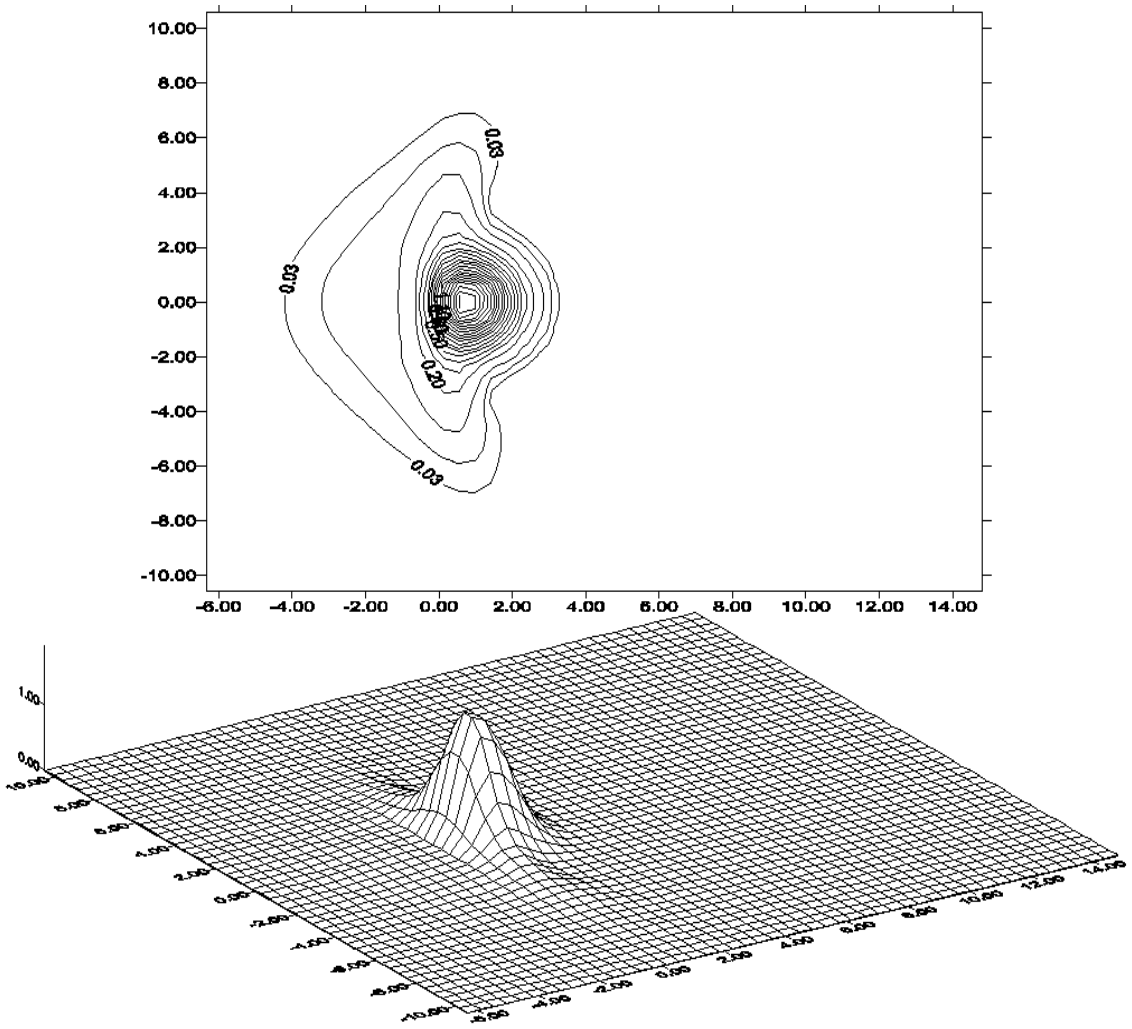

FIGURE 10. Distribution Function $f(\xi_x, \xi_y, \xi_z, x, y)$ at $x = 4\lambda, y = 0.25\lambda$, $\xi_z = h/2$